A New Color Image Zooming Technique for Digital Still Cameras

R. Lukac[1], *K.N. Plataniotis*[1], *B. Smolka*[2], and *D. Hatzinakos*[1]
[1] *The Edward S. Rogers Sr. Department of ECE, University of Toronto*
Toronto, Ontario, Canada
[2] *Silesian University of Technology, Laboratory of Multimedia Communication*
Rybnik, Poland

Abstract

This paper focuses on color image zooming performed on the Bayer pattern, a color filter array widely used in digital still cameras. The proposed method firstly enlarges the Bayer image and secondly interpolates the missing color elements of the enlarged Bayer image by an edge-sensing interpolation scheme combined with a color difference model. This enhances structural content preservation and results in excellent color fidelity of the enlarged image. The proposed edge-sensing zooming algorithm preserves the structural content of the Bayer data and produces a sharp, enlarged output. Used cascades of the proposed zooming method and efficient color filter array interpolations produce images that are naturally colored and pleasurable for viewing. This also results in excellent results in terms of objective image quality measure.

Introduction

Single-sensor digital color cameras acquire color information by transmitting the image through a color filter array (CFA) and then sampling visual information using an electronic sensor, usually charge coupled devices (CCD) and complementary metal oxide semiconductor (CMOS) sensors. The Bayer pattern (Figure 1a),[2] a widely used CFA, provides the array or mosaic of the Red (R), Green (G) and Blue (B) colors so that only one color element is available in each pixel. The process of estimating the two missing color components from the adjacent pixels is called CFA interpolation.[6]

The spatial resolution of the acquired color images can be increased in two ways, namely: i) restored image zooming, and ii) CFA image zooming. The first approach interpolates missing CFA image colors using a CFA interpolation scheme and then enlarges the spatial resolution of the restored images. Missing color pixels in the resampled images are estimated using the appropriate method. Zooming efficiency of this approach mainly depends on the CFA interpolation efficiency, because most of CFA interpolation approaches introduce an initial inaccuracy in the form of blurred edges and false colors.[6] Increasing the spatial resolution of such a restored image means that missing image pixels are often estimated from these inaccurate estimates. This results in visual impairing of enlarged images. Therefore, the choice of the efficient demosaicing techniques is of paramount importance. The CFA interpolation methods have been surveyed in Ref. [6].

A novel approach to zooming operates directly on the CFA data.[5] Applying a CFA interpolation technique the enlarged color image is constituted form the Bayer image with the increased spatial resolution. Bayer pattern zooming was also studied[3,4] where a locally adaptive zooming algorithm combined with a simple interpolation technique such as the bilinear or bicubic interpolation was introduced. Enlarging directly on the Bayer pattern and consequently restoring the enlarged Bayer pattern using a CFA interpolation scheme, the algorithms of Ref. [4] led to restored color images of acceptable quality.

Proposed Method

The proposed here method firstly enlarges the Bayer pattern and secondly interpolates the missing color elements by an edge-sensing interpolation scheme. Instead replicating CFA pixels in four sub-pixels of Refs. [3] and [4], a new method assigns original CFA pixels to unique positions in the enlarged CFA image. Missing pixels of the CFA image with the increased spatial resolution are interpolated. To follow varying image statistics and changes in structural information of the image, the proposed adaptive scheme utilizes an edge-sensing mechanism combined with a color difference model. This enhances structural content preservation and results in excellent color fidelity of the enlarged image.

Let us consider a $K_1/k \times K_2/k$ Bayer image $z'(i): Z^2 \to Z$ and spatial coordinates p,q characterizing the image row and column. Zooming the Bayer data $z'(i)$ with a factor of k, this process results in a $K_1 \times K_2$ zoomed Bayer image $z(i): Z^2 \to Z$. The zooming factor k can be arbitrary, however; the value $k = 2$ is selected here for demonstration purposes to facilitate the discussion. Note that a zooming procedure with a factor of 2 first enlarges the original image and then incorporates new rows and columns (e.g. of zeros) into the original image. Operating on the Bayer data in this way destroys the structure of the Bayer pattern, since original values often occupy spatial positions corresponding to other color channels (Figure 1b).

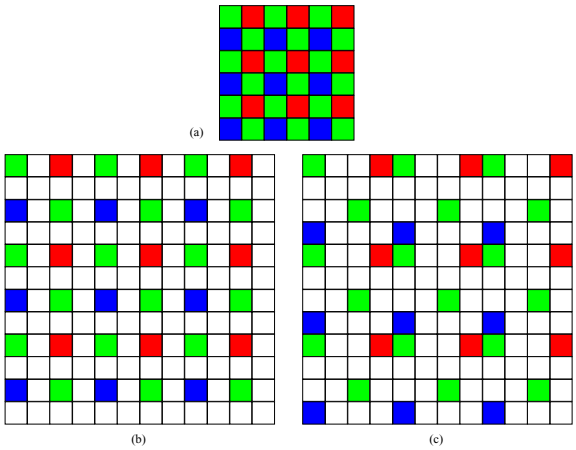

Figure 1. Bayer CFA pattern (a) and Bayer patter zooming (b,c) by: (b) standard approach, which destroys the structure of the Bayer pattern (color elements do not correspond to Bayer color positions), (c) proposed method cont. in Figure 2.

To zoom the Bayer data and preserve the Bayer pattern structure, original CFA data should assign unique positions[5] in the enlarged CFA image shown in Figure 1c. Filling the values in the enlarged Bayer image, it is necessary to distinguish the spatial positions of estimated samples, especially the spatial/structural closeness between the R,G and G,B values in the enlarged image. It can be seen that most of samples of the original image $z'(i)$ create in the zoomed image $z(i)$ the RGB triplets with the center in G values. This means that these spatially closer relationships have to be reflected in the interpolation of missing G values neighboring with the triplet R and B values. Thus, based on the structural information of the original Bayer image, we estimate the G value positioned in the B center of four original G values as follows:

$$z_{(2p-1,2q-1)} = \left(\sum_{j=1}^{4} w_j z'_j\right) / \left(\sum_{j=1}^{4} w_j\right) \tag{1}$$

where p,q (for p even and q odd) denotes the spatial position on the original Bayer image, $z'_1, z'_2, ..., z'_4$ are averaged values given by

$$z'_1 = (z'_{(p-1,q)} + z'_{(p+1,q)})/2 \tag{2}$$

$$z'_2 = (z'_{(p,q-1)} + z'_{(p,q+1)})/2 \tag{3}$$

$$z'_3 = (z'_{(p-1,q)} + z'_{(p,q-1)})/2 \tag{4}$$

$$z'_4 = (z'_{(p-1,q)} + z'_{(p,q+1)})/2 \tag{5}$$

where the triple use of $z'_{(p-1,q)}$ in (2), (4) and (5) reflects the spatial closeness of the B center $z'_{(p,q)}$ and the G value $z'_{(p-1,q)}$ positioned above $z'_{(p,q)}$. Due to the proposed concept shown in Figure 1c, samples $z'_{(p,q)}$ and $z'_{(p-1,q)}$ are also neighbors in the enlarged image $z(i)$. This property is not satisfied for other neighboring original G values $z'_{(p+1,q)}$, $z'_{(p,q-1)}$ and $z'_{(p,q+1)}$.

The same idea is also taken by the edge-sensing weight coefficients $w_1, w_2, ..., w_4$ of (1) are given by

$$w_1 = 1/\left(1 + \left|z'_{(p-1,q)} - z'_{(p+1,q)}\right|/2\right) \tag{6}$$

$$w_2 = 1/\left(1 + \left|z'_{(p,q-1)} - z'_{(p,q+1)}\right|/2\right) \tag{7}$$

$$w_3 = \frac{\left|z'_{(p-1,q)} + z'_{(p,q-1)} - z'_{(p+1,q)} - z'_{(p,q+1)}\right|}{\xi + \left|z'_{(p-1,q)} + z'_{(p,q-1)} - z'_{(p+1,q)} - z'_{(p,q+1)}\right|} \tag{8}$$

$$w_4 = \frac{\left|z'_{(p-1,q)} + z'_{(p,q+1)} - z'_{(p+1,q)} - z'_{(p,q-1)}\right|}{\xi + \left|z'_{(p-1,q)} + z'_{(p,q+1)} - z'_{(p+1,q)} - z'_{(p,q-1)}\right|} \tag{9}$$

where ξ is the threshold value, which controls the edge sensitivity. When ξ is fairly small, the edge mechanism detects even small contrasts. For high ξ, some edges can pan undetected. Experimentation with a wide range of natural images indicate that a value $\xi = 15$ can be used in conjunction with the weights of (8) and (9). The above-described interpolation step vertically surrounds original B values with two G values (Figure 2a).

Similarly, we can estimate the G values positioned in the R center of four original G values. Since the proposed zooming concept transforms the original R sample $z'_{(p,q)}$ and original G samples $z'_{(p-1,q)}, z'_{(p+1,q)}, z'_{(p,q-1)}, z'_{(p,q+1)}$ in the way that $z'_{(p,q)}$ and $z'_{(p,q+1)}$ are spatially neighboring in the enlarged image $z(i)$, the variable of (4) has to be redefined as follows:

$$z'_3 = (z'_{(p,q+1)} + z'_{(p+1,q)})/2 \tag{10}$$

whereas (2), (3) and (5) remain unchanged. Since the weight coefficients of (6) to (9) employ required relationships, they remain unchanged as well. Thus, eq. (1) with supports of (10) and previously defined quantities horizontally surrounds original R values with the two G values as shown in Figure 2b.

Since the rest of missing CFA samples of the enlarged image $z(i)$ are positioned in the neighborhood of original samples of $z'(i)$ and previously interpolated G values of $z(i)$, it is not surprising to interpolate them with the simultaneous use of original and interpolated values. Therefore, to facilitate the following steps it is necessary to operate on the enlarged image $z(i)$.

Operating on the $K_1 \times K_2$ enlarged Bayer image $z(i)$ with spatial coordinates p,q and using the averaging concept applied to diagonally positioned G values, the G values in B rows associated with spatial positions $p = 2,6,10,..., K_1 - 2$, $q = 2,6,10,..., K_2 - 2$ and $p = 4,8,12,..., K_1$, $q = 4,8,12,..., K_2$ respectively, are interpolated as follows:

$$z_{(p,q)} = \left(\sum_{j=1}^{4} w_j z_j\right) / \left(\sum_{j=1}^{4} w_j\right) \tag{11}$$

where $z_1, z_2, ..., z_4$ are defined using the values of $z(i)$:

$$z_1 = (z_{(p-1,q-1)} + z_{(p-1,q+1)})/2 \tag{12}$$

$$z_2 = (z_{(p-1,q-1)} + z_{(p+1,q-1)})/2 \tag{13}$$

$$z_3 = (z_{(p-1,q+1)} + z_{(p+1,q-1)})/2 \tag{14}$$

$$z_4 = (z_{(p-1,q-1)} + z_{(p+1,q+1)})/2 \tag{15}$$

This way is appropriate, since the referred, spatially most important CFA pixel to $z_{(p,q)}$ is now positioned as the sample $z_{(p-1,q-1)}$. Corresponding weight coefficients $w_1, w_2, ..., w_4$ are given by

$$w_1 = \frac{\left|z_{(p-1,q-1)} + z_{(p-1,q+1)} - z_{(p+1,q+1)} - z_{(p+1,q+1)}\right|}{\xi + \left|z_{(p-1,q-1)} + z_{(p-1,q+1)} - z_{(p+1,q-1)} - z_{(p+1,q+1)}\right|} \tag{16}$$

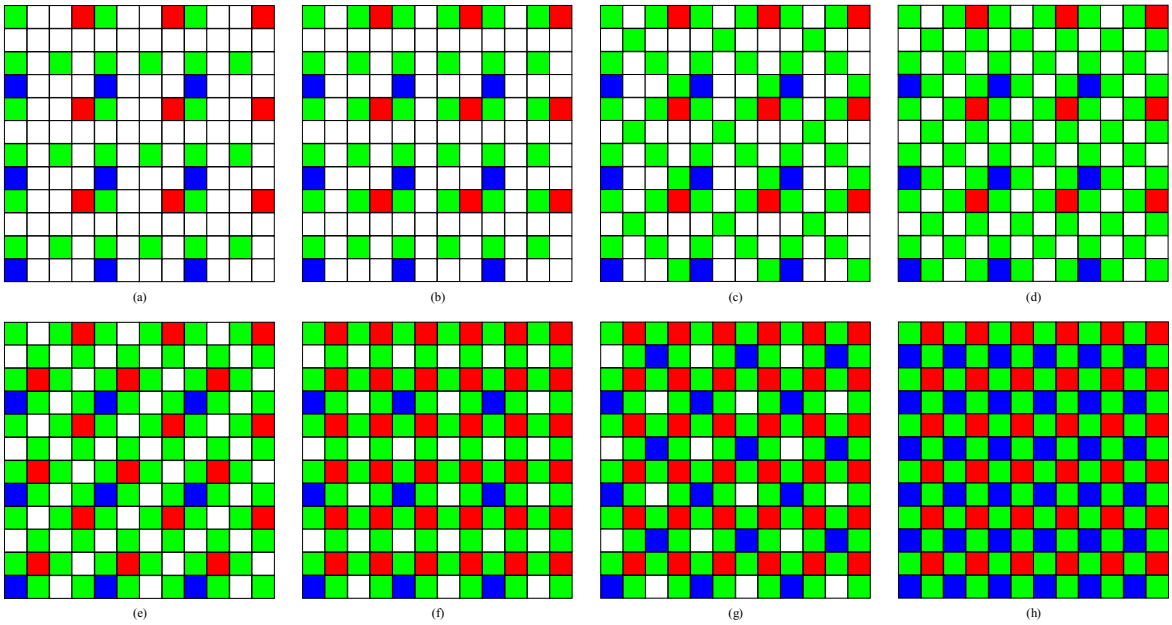

Figure 2. Proposed interpolation of color elements in the zoomed Bayer pattern.

$$w_2 = \frac{\left|z_{(p-1,q-1)} + z_{(p+1,q-1)} - z_{(p-1,q+1)} - z_{(p+1,q+1)}\right|}{\xi + \left|z_{(p-1,q-1)} + z_{(p+1,q-1)} - z_{(p-1,q+1)} - z_{(p+1,q+1)}\right|} \quad (17)$$

$$w_3 = 1/\left(1 + \left|z_{(p-1,q-1)} - z_{(p+1,q-1)}\right|/2\right) \quad (18)$$

$$w_4 = 1/\left(1 + \left|z_{(p-1,q-1)} - z_{(p+1,q+1)}\right|/2\right) \quad (19)$$

where ξ is the same threshold value as in (8) and (9). This interpolation step results in Figure 2c.

The rest of the G values in B rows associated with spatial positions $p = 2,6,10,...,K_1 - 2$, $q = 4,8,12,...,K_2$ and $p = 4,8,12,...,K_1$, $q = 2,6,10,...,K_2 - 2$, respectively, are also estimated using (11) with z_2 redefined as follows:

$$z_2 = (z_{(p-1,q+1)} + z_{(p+1,q+1)})/2 \quad (20)$$

This equation reflects the importance of $z_{(p-1,q+1)}$ used as the reference, spatially most important sample to $z_{(p,q)}$. This interpolation step results in the completely filled G channel of $z(i)$ (Figure 2d).

In the next step, the zooming process continues with interpolation of the R values associated with spatial coordinates $p = 3,7,11,...,K_1 - 1$ and $q = 2,6,10,...,K_2 - 2$. The purpose of this step is to fill the R values in the center of four surrounding original R values. Because the original R values are not positioned in the nearest neighborhood of the estimated R values, the proposed interpolation scheme utilizes the difference model,[1] taking advantage of its simplicity and efficiency. Adopting the difference model, eq. (11) is modified as follows:

$$z_{(p,q)} = z_{(p,q-1)} + \left(\sum_{j=1}^{4} w_j z_j\right) / \left(\sum_{j=1}^{4} w_j\right) \quad (21)$$

where $z_{(p,q-1)}$ is the G value spatially closest to $z_{(p,q)}$ and $z_1, z_2, ..., z_4$ are color difference quantities defined by

$$z_1 = (z_{(p-2,q-2)} - z_{(p-2,q-3)} + z_{(p-2,q+2)} - z_{(p-2,q+1)})/2 \quad (22)$$

$$z_2 = (z_{(p-2,q+2)} - z_{(p-2,q+1)} + z_{(p+2,q+2)} - z_{(p+2,q+1)})/2 \quad (23)$$

$$z_3 = (z_{(p-2,q-2)} - z_{(p-2,q-3)} + z_{(p+2,q+2)} - z_{(p+2,q+1)})/2 \quad (24)$$

$$z_4 = (z_{(p-2,q+2)} - z_{(p-2,q+1)} + z_{(p+2,q-2)} - z_{(p+2,q-3)})/2 \quad (25)$$

Corresponding weights are determined analogously to previous definitions of (16) to (19), however with a simple replacement of $z_{(p-1,q-1)}, z_{(p+1,q-1)}, z_{(p-1,q+1)}, z_{(p+1,q+1)}$ with $z_{(p-2,q-2)}, z_{(p+2,q-2)}, z_{(p-2,q+2)}, z_{(p+2,q+2)}$. Thus, eq. (21) produces the image shown in Figure 2e.

The rest of the R values for $p = 1,5,9,...,K_1 - 3$, $q = 2,6,10,...,K_2 - 2$ and $p = 3,7,11,...,K_1 - 1$, $q = 4,8,12,...,K_2$, respectively, is estimated in one pass as follows:

$$z_{(p,q)} = z_{(p,q+1)} + \left(\sum_{j=1}^{4} w_j z_j\right) / \left(\sum_{j=1}^{4} w_j\right) \quad (26)$$

where $z_{(p,q+1)}$ is the interpolated G value and $z_1, z_2, ..., z_4$ are color difference quantities (differences between original R values and interpolated G values) defined by

$$z_1 = (z_{(p-2,q)} - z_{(p-2,q-1)} + z_{(p+2,q)} - z_{(p+2,q-1)})/2 \quad (27)$$

$$z_2 = (z_{(p,q-2)} - z_{(p,q-3)} + z_{(p,q+2)} - z_{(p,q+1)})/2 \quad (28)$$

$$z_3 = (z_{(p-2,q)} - z_{(p-2,q-1)} + z_{(p,q+2)} - z_{(p,q+1)})/2 \quad (29)$$

$$z_4 = (z_{(p-2,q)} - z_{(p-2,q-1)} + z_{(p,q-2)} - z_{(p,q-3)})/2 \quad (30)$$

Corresponding weight coefficients are given by

$$w_1 = 1/\left(1 + \left|z_{(p-2,q)} - z_{(p+2,q)}\right|/2\right) \quad (31)$$

$$w_2 = 1/\left(1 + \left|z_{(p,q+2)} - z_{(p,q-2)}\right|/2\right) \quad (32)$$

$$w_3 = \frac{\left|z_{(p-2,q)} + z_{(p,q+2)} - z_{(p,q-2)} - z_{(p+2,q)}\right|}{\xi + \left|z_{(p-2,q)} + z_{(p,q+2)} - z_{(p,q-2)} - z_{(p+2,q)}\right|} \quad (33)$$

$$w_4 = \frac{\left|z_{(p-2,q)} + z_{(p,q+2)} - z_{(p,q+2)} - z_{(p+2,q)}\right|}{\xi + \left|z_{(p-2,q)} + z_{(p,q+2)} - z_{(p,q+2)} - z_{(p+2,q)}\right|} \qquad (34)$$

Using the estimation procedure of (26), the R values are fully interpolated as shown in Figure 2f.

Since R values are symmetrically positioned to the B values, interpolation of the B channel is practically identical with the R channel interpolation. Assuming that q denotes the image row, whereas p characterizes the image column, eq. (21) can be used in straightforward way also for interpolation of the B values as shown in Figure 2g. Consecutively, the rest of B values are obtained using (26). This interpolation steps results in the fully interpolated, enlarged Bayer data $z(i)$ shown in Figure 2h and thus it also concludes the introduced zooming algorithm for Bayer CFA image.

Figure 3. Test color images.

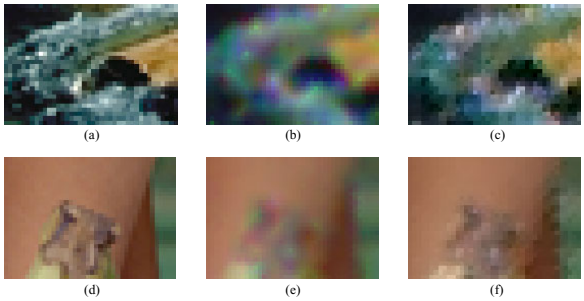

Figure 4. Zoomed parts of the test images: (a,d) original image, (b,e) BCZ + BI, (c,f) Proposed zooming + CCA.

Experimental Results

The proposed zooming method is tested using the color test images of the database shown in Figure 3. This database is widely used for CFA interpolation purposes, because: i) it contains natural, real life images, ii) similar color scenarios can be captured by camera users and, iii) these images vary in complexity and color appearance. Note that all test images have the same size of 512×512 pixels with a 8-bit per channel RGB representation.

To measure the efficiency of the zooming methods objectively, we used the following approach. The process starts with the $K_1\times K_2$ original color image $\mathbf{o}(i)$ down-sampled to $K_1/2\times K_2/2$ color image. This image is transformed into the $K_1/2\times K_2/2$ Bayer image $z'(i)$. Using a variety of zooming methods we can constitute the zoomed $K_1\times K_2$ Bayer image $z(i)$. Applying any CFA interpolation method, this process results in the $K_1\times K_2$ interpolated RGB image $\mathbf{y}(i)$. In this paper, the closeness between $\mathbf{o}(i)$ and $\mathbf{y}(i)$ is measured[7] by the mean absolute error (MAE), the mean square error (MSE) and the normalized difference criterion (NCD).

To compare the efficiency of method, we will make use of bicubic zooming (BCZ), locally adaptive zooming (LAZ)[4] and proposed zooming (PZ); cascaded with CFA interpolation methods such as bilinear interpolation (BI) and correlation-correction approach (CCA).[6]

Table 1. Averaged results corresponding to Figure 3

Method	MAE	MSE	NCD
BCZ + BI	10.83	422.75	0.1207
LAZ + BI	10.89	425.29	0.1151
PZ + BI	8.93	288.30	0.0944
BCZ + CCA	10.51	388.56	0.1007
LAZ + CCA	10.49	386.18	0.0969
PZ + CCA	8.64	264.66	0.0887

Conclusion

A new Bayer CFA data zooming method was presented. Combining advantages of edge sensing mechanism and difference color model, the proposed zooming method followed by the efficient CFA interpolation method avoids color artifacts and produces enlarged color images pleasurable for viewing.

References

1. J. Adams, Design of Practical Color Filter Array Interpolation Algorithms for Digital Cameras, Proc. of the SPIE, 3028, pp. 117-125 (1997).
2. B.E. Bayer, Color Imaging Array, U.S. Pat 3 971 065.
3. S. Battiato, M. Guarnera, M. Mancuso, and A. Bruna, Bayer Image Enlargement Using Correlated Color Components, Proc. Internat. Conf. on Consumer Electronics ICCE'02, pp. 230-231, (2002).
4. S. Battiato, G. Gallo, and F. Stanco, A Locally Adaptive Zooming Algorithm for Digital Images," Image and Vision Computing, 20, pp. 805-812, (2002).
5. R. Lukac and K.N. Plataniotis, Digital Camera Zooming on the Colour Filter Array, IEE Electronic Letters, 39, pp.1806-1807, (2003).
6. R. Lukac, K.N. Plataniotis, D. Hatzinakos, and M. Aleksic, A New CFA Interpolation Framework, Signal Processing, submitted for publication (2003).
7. K.N. Plataniotis and A.N. Venetsanopulos, Color Image Processing and Applications, Springer-Verlag, Berlin, (2000).

Biography

Rastislav Lukac received a Diploma in Telecommunications with honors in 1998 and a Ph.D. in 2001, both at the Technical University of Kosice, Slovak Republic. From February 2001 to August 2002 he was an assistant professor at the Department of Electronics and Multimedia Communications at the Technical University

of Kosice. Since August 2002 he is a researcher in Slovak Image Processing Center in Dobsina, Slovak Republic. From January 2003 to March 2003 he was a post-doc at Artificial Intelligence & Information Analysis Lab at the Aristotle University of Thessaloniki, Greece. In 2003, he was awarded the NATO Science Fellowship. Since May 2003 he has been a post-doctoral fellow at the Edward S. Rogers Sr. Department of Electrical and Computer Engineering at the University of Toronto in Toronto, Canada. e-mail: lukacr@ieee.org, kostas@dsp.utoronto.ca